Functionalised metal-organic frameworks

A novel approach to stabilising single metal atoms

Szilágyi, P.; Rogers, D. M.; Zaiser, I.; Callini, E; Turner, Stuart; Borgschulte, A; Züttel, A.; Geerlings, H.; Hirscher, M; Dam, B.

DOI
10.1039/c7ta03134c

Publication date
2017

Document Version
Accepted author manuscript

Published in
Journal of Materials Chemistry A

Citation (APA)
Szilágyi, P., Rogers, D. M., Zaiser, I., Callini, E., Turner, S., Borgschulte, A., Züttel, A., Geerlings, H., Hirscher, M., & Dam, B. (2017). Functionalised metal-organic frameworks: A novel approach to stabilising single metal atoms. *Journal of Materials Chemistry A*, *5*(30), 15559-15566. https://doi.org/10.1039/c7ta03134c

Accepted Author Manuscript of http://dx.doi.org/10.1039/c7ta03134c

Journal of Materials Chemistry A

PAPER

Functionalised metal-organic frameworks: a novel approach to stabilising single metal atoms

Received 00th January 20xx,
Accepted 00th January 20xx

DOI: 10.1039/x0xx00000x

www.rsc.org/

P. Á. Szilágyi[a,b*], D. M. Rogers[c], I. Zaiser[d], E. Callini[e,f], S. Turner[g], A. Borgschulte[e], A. Züttel[e,f], H. Geerlings[d,h], M. Hirscher[d] and B. Dam[b]

We have investigated the potential of metal-organic frameworks for immobilising single atoms of transition metals using a model system of Pd supported on NH_2-MIL-101(Cr). Our Transmission Electron Microscopy and *in-situ* Raman spectroscopy results give evidence for the first time that functionalised metal-organic frameworks may support, isolate and stabilise single atoms of palladium. Using Thermal Desorption Spectroscopy we were able to evaluate the proportion of single Pd atoms. Furthermore, in a combined theoretical-experimental approach, we show that the H-H bonds in a H_2 molecule elongate by over 15% through the formation of a complex with single atoms of Pd. Such deformation would affect any hydrogenation reaction and thus the single atoms supported on metal-organic frameworks may become promising single atom catalysts in the future.

Introduction

Specific activity and selectivity of heterogeneous catalysts improve with decreasing particle sizes owing to an increased surface-to-volume ratio and limited numbers of neighbouring atoms [1] and thus the development of synthetic approaches to decrease the particle size of transition metals has been in the forefront of materials science and chemical engineering in the past decade. [1b;2] The ultimate size limit for metal particles is the single atom which, with the recognition of single atom catalysts (SACs), have become the focus of scientific attention. [3] To date however, reliable methods for the isolation and stabilisation, or immobilisation of single atoms of various transition metals, and approaches for their quantification remain challenging.

Current technology for the isolation and stabilisation of single metal atoms offers two fundamentally different approaches; the first one is formed through primary bonds of the transition-metal atom with ligands such as CO [4], whereas the second approach makes use of strong secondary interactions between the metal atom and typically a 2D substrate, such as metal oxides. [3a;5] While the formation of complexes with single metal atoms completely changes the electronic structure and thus the chemistry of the metals [4c-e;6], 2D substrates effectively allow the isolation of single atoms. They however also have serious drawbacks; *i)* the binding sites cannot be fully controlled, which allows for the diffusion and agglomeration, or sintering of the metal atoms into clusters and nanoparticles [3b;5a]; *ii)* the support may encapsulate the single atoms, effectively depleting the concentration of the transition metal [7]; and *iii)* very strong metal-support interactions could potentially stabilise the single atoms thereby decreasing their catalytic activity. [8]

In this work we put forward a third approach to isolating and stabilising single atoms of transition metals, which combines elements of the above two methods. We postulate that metal-organic frameworks (MOFs) are a desirable and useful chemical support for immobilising single atoms of transition metals. MOFs are a relatively new class of materials typically built up of metal oxide polyhedra interconnected by organic linkers. They are highly crystalline and display high and regular porosity. [9] MOFs boast of unprecedented large specific surface areas. [9;10] They have been highlighted for their potential to incorporate catalytically active species, such as coordinatively unsaturated ionic sites [11] and they have also shown much promise as supporting matrices of heterogeneous catalyst particles, which highlights their potential to rival conventional 2D supports. [12] Furthermore, their inherently rich chemistry does not solely extend to the hybrid nature of their building blocks but also allows for the introduction of

[a] University of Greenwich, Department of Pharmaceutical, Chemical and Environmental Sciences, Chatham Maritime, ME4 4TB, UK
[b] Delft University of Technology, Department of Chemical Engineering, Julianalaan 136, 2628BL Delft, Netherlands
[c] School of Chemistry, The University of Edinburgh, Joseph Black Building, The King's Buildings, David Brewster Road, Edinburgh, EH9 3FJ, UK
[d] Max Planck Institute for Intelligent Systems, Heisenbergstrasse 3, 70569 Stuttgart, Germany
[e] Swiss Federal Laboratories for Materials Science and Technology, EMPA, Überlandstrasse 129, CH-8600 Dübendorf, Switzerland
[f] École Polytechnique de Lausanne, EPFL Valais/Wallis, ISIC, LMER, rue de l'industrie 17, 1950 Sion, Switzerland
[g] Electron Microscopy for Materials Science, EMAT, Groenenborgerlaan 171, 2020 Antwerp, Belgium
[h] Shell Technology Centre, Grasweg 31, 1031 HW Amsterdam, Netherlands
*Author to whom correspondence should be sent: P.A.Szilagyi@greenwich.ac.uk
† Electronic Supplementary Information (ESI) available: [details of any supplementary information available should be included here]. See DOI: 10.1039/x0xx00000x

further functionalities on both the organic [13] and inorganic [14] sides. This property may enable the coordination of single transition-metal atoms to functional groups, mimicking atomic transition-metal complexes. Regardless, to date no single 'naked' metal atoms, *i.e.* neutral isolated single particles have been stabilised and observed in a metal-organic framework. This is particularly important as there is a persistent inaccuracy in the literature of referring to charged metal ions as atoms, the latter of which typically have much lower stability than their charged counterparts and therefore are much more challenging to obtain as single entities. [15]

The characterisation of composite materials of dispersed single metal atoms is highly complex. While it is crucial to obtain high-quality and high-definition micrographs capable of demonstrating the presence of single atoms, *cf.* using transmission-electron microscopy, it is impossible to quantify the concentration of these atoms in the sample based solely on these micrographs. [12a&c] Furthermore, practical evidence shows that regardless of the synthetic approach, sintering of the metal atoms into nanoparticles always occurs to some extent [3b;5a], and therefore the bulk quantification, *cf.* inductively-coupled plasma mass spectrometry/optical emission spectroscopy (ICP-MS/OES), of the transition metal within the sample will not accurately reflect the concentration of single metal atoms present in the matrix.

In order to address the above issues of characterisation, we have carried out a series of complementary experiments to *i)* verify the presence of single transition-metal atoms using transmission electron microscopy and *ii)* estimate the quantity of the single atoms with the help of thermal desorption spectroscopy, also supported with density functional theory and *in-situ* Raman spectroscopy.

It should be emphasised that while MOFs have been shown to successfully immobilise single ions or embed nanoparticles of transition metals [12;15], to date no experimental evidence of single 'naked' (neutral) atoms supported on a MOF has been given. This highlights both the usefulness of this class of materials as supports and the challenges related to immobilise single atoms, particularly when considering that single ions are less likely to sinter on account of their electric charge.

Results and discussion

For our experiments we chose to focus on embedding atomic Pd in the pores of a MOF structure (NH_2-MIL-101(Cr)). In such a system we expect the formation of $Pd(H_2)$, where a single Pd atom is bonded to a H_2 molecule whilst the H-H bond remains unbroken. This is a suitable model system as its reversible operation requires relatively mild conditions, and it has distinctive Raman and IR features. [16]

While MOFs have been highlighted as promising matrices for embedding nanoparticles and nanoclusters of transition metals [12], it has also been shown that in some cases it is energetically more preferable for the metal to form larger particles on the MOF surface. [17] This phenomenon has been rationalised recently in terms of the relationship between the adsorption enthalpy of the metal atoms and their affinity to form clusters. [18] It has also been calculated and experimentally confirmed that it is possible for neutral Pd atoms to form coordinate bonds with $–NH_2$ groups on the MOF linker, ensuring a strong interaction between the MOF matrix and the Pd atoms. [18]

Using this input we postulated that if a non-functionalised MOF is adequate for the embedding of nanoparticles, it follows that a functionalised isoreticular MOF should bind to the transition-metal atoms more strongly, possibly strong enough to immobilise them. Previously, it has been shown that the MIL-101(Cr) [19] framework is an excellent matrix for supporting Pd nanoparticles in an appreciable range of temperature and applied gas pressure [20], which suggests a reasonably strong host-guest interaction. In addition, MIL-101(Cr) is susceptible to partial linker exchange [21], which can be exploited to control the amount of functional groups available. Previously it has been shown that amino functionalisation of a MOF increases the binding energy of Pd on the MOF. Therefore we selected the NH_2-MIL-101(Cr) [22] framework to stabilise single Pd atoms on. It should be noted that Pd nanoparticles have been successfully embedded previously in the pores of NH_2-MIL-101(Cr) with very high Pd loading (8 wt%) [23], which favours the formation of nanoparticles rather than single 'naked' atoms, it is for this reason that we aimed at keeping the amount of Pd added low. Fourier Transformation Infrared (FTIR) spectra (ESI, Figure S1) were acquired on the sample in its three preparation stages; an initial control spectrum was acquired on the empty or unloaded NH_2-MIL-101(Cr), which was compared with that acquired after the addition of the Pd precursor, $Pd(CH_3COO)_2$. Finally, a third FTIR spectrum was recorded after the reduction of the Pd precursor. N.B. during the reduction step the acetate counter-anions were removed as volatile products. The N-H stretching modes have been found to undergo a discernible, 4 cm^{-1}, blueshift upon the addition of $Pd(CH_3COO)_2$, as a result of the formation of a Pd(II)←:NH_2- coordinate bond, which further polarises the N-H bond, similarly to the analogous $[Pd(NH_3)_4]^{2+}$. [24] The spectrum acquired after the reduction of Pd on the other hand, displays rather complex spectral

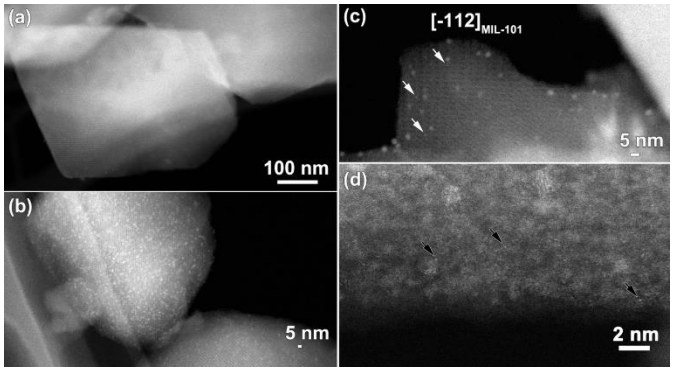

Figure 1 HAADF-STEM images of the Pd containing NH_2-MIL-101(Cr) (a) low-magnification image, showing the faceted shape of the MIL-101 crystals; (b) medium-magnification image showing the presence of well-dispersed Pd clusters; (c) high-magnification image showing a MIL-101 crystal imaged along the [-112] zone axis. The Pd particles (examples indicated by white arrows) are max. 3 nm in diameter and (d) atomic resolution HAADF-STEM image, showing the presence of individual Pd atoms (examples indicated by black arrows)

features, suggesting that some of the $–NH_2$ groups are still in close contact with the Pd whereas others are not, possibly due to partial agglomeration of the Pd atoms. This observation is in line with what would be expected from strong host-guest interactions such as those needed for immobilising single Pd atoms. The strength of the Pd-MOF bonds is also underlined by the slight oxidation shift of Pd observed in the X-ray Photoelectron Spectroscopy (XPS) spectrum (ESI, Figure S2), consistent with a persisting interaction of the Pd atoms with the amino groups of the framework. [18]

More importantly, High-Angle Annular Dark-Field Scanning Transmission Electron Microscopy (HAADF-STEM) micrographs (Figure 1) reveal that, while the agglomeration of Pd atoms could not be completely avoided (Figure 1b and c), for the first time atomic resolution images show the presence of a substantial amount of single atoms in the pores of a MOF (NH_2-MIL-101(Cr), Figure 1d).

In addition, according to previous literature that pores on the surface of MOF particles are preferentially filled [25], our HAADF-STEM tomography images however revealed that Pd is uniformly distributed throughout the NH_2-MIL-101(Cr) particles (ESI, Figure S3), a significant improvement for applications.

The presence of both single atoms and nanoparticles of Pd highlights the difficulty in determining the proportion of the Pd single atoms, as the 0.85% Pd content, measured by ICP-OES, includes contributions from both.

However, as only single atoms of Pd form the $Pd(H_2)$ complex under H_2 gas pressure, the detection and quantification of this complex may help *i)* further confirm the presence of the single atoms of Pd and *ii)* estimate their proportion. In order to verify the formation of the $Pd(H_2)$ complex, we have acquired *in-situ* Raman spectra under 20 bar pressure of H_2 and D_2 (ESI, Figure S4). The results obtained are in excellent agreement with previous matrix infrared results [16] and our computational modelling of the system (ESI, Table S1-S3). From the Raman spectra it is apparent that it is the $Pd(H_2)$ complex, not the immobilised -(NH_2)-Pd-(H_2) species, which is formed when the sample is exposed to 20 bar hydrogen pressure. On the other hand our *ex-situ* FTIR results show that the single Pd atoms are immobilised on the -NH_2 functional groups of the framework, which in turn would change the electronic structure of the Pd atom thereby changing the spectral characteristics of the $Pd(H_2)$ complex. To reconcile this contradiction we have performed further DFT calculations using a model system of a single Pd atom bonded to ammonia, which represents the amino functional group of the framework. The hydrogenation of this H_3N-Pd species was modelled and it was found that it would yield a transition-state species of H_3N-$Pd(H_2)$. Owing to the transitional nature of the hydrogenated adduct H_3N-$Pd(H_2)$ the H_3N-Pd species spontaneously decomposes when exposed to H_2 pressure according to the below reaction (Eq. 1), with a reaction enthalpy of −3.65 kJ mol^{-1} and net free energy change of −10.75 kJ mol^{-1}.

$$H_3N\text{-}Pd(H_2) \rightarrow NH_3 + Pd(H_2) \qquad \text{(Eq. 1)}$$

This spontaneous reaction is therefore the reason why the formation of 'naked' $Pd(H_2)$ is detected when a starting material, in which single atoms are immobilised on amino groups, is exposed to hydrogen pressure.

This elongation corresponds to a significant activation, or destabilisation of the H-H bonds, which can have very important consequences in hydrogenation reactions highlighting the potential of these metal-MOF composites as single atom catalysts. Supported SACs blur the difference between homogeneous and heterogeneous catalysis as they participate intimately in reactions, however they also are dispersed on a supporting matrix of a different phase so they may potentially offer unprecedented opportunities for catalysis. A recent example of supported SACs, in particular in hydrogenation reactions, made use of single Pt atoms supported on phosphomolybdic acid (PMA)-modified active carbon, which showed superior performance in the hydrogenation of nitrobenzene and cyclohexanone. [27]

Table 1 Formation reactions of the $Pd(H_2)$ complex from constituent single palladium atom and hydrogen molecule; molecular structure including bond lengths and angles, and the enthalpy and free energy change of said reaction obtained from DFT calculations at standard-conditions.

Reaction	Structure	Reaction enthalpy (kJ mol^{-1})	Free energy change of reaction (kJ mol^{-1})
Pd ($^1A_{1G}$) + H_2 ($^1\Sigma_g$) → $Pd(H_2)$ ($^1A_1$)		−83.32	−60.32

To be able to appreciate the proportion of Pd single atoms supported on the NH_2-MIL-101(Cr) framework, one may make use of its reaction with hydrogen, as observed using *in-situ* Raman spectroscopy. However, hydrogen is also chemisorbed by the Pd nanoparticles through the formation of the β-phase hydride $PdH_{0.67}$, since the applied hydrogen pressure was well above the plateau pressure. Hence, the observed increase in the MOF's hydrogen uptake after the embedment of Pd has been inconclusive. The increased uptake at low hydrogen loading in the Pd-containing sample (ESI, Figure S4) reveals the formation of more strongly bonding absorption sites than those in the bare MOF. These new sites could correspond to both a small amount of interstitial hydrogen in the α-phase Pd nanoparticles as well as the hydrogen adsorbed on the single Pd atoms. [16;20;28] Taking into consideration the low Pd concentration in the MOF and the potential error of the hydrogen-isotherm measurements it becomes apparent that a more accurate method needs to be employed to determine the proportion of Pd single atoms.

While the quantity of hydrogen absorbed does not allow for the determination of the single-atom fraction (ESI, Figure S5), the enthalpy of hydrogen adsorption on the two different Pd species, *i.e.* single atoms and nanoparticles, is remarkably different. This difference arises from the distinct bonding principles. While Density Functional Theory (DFT) calculations (see [16] and ESI, Table S1-S3) show that two different $Pd(H_2)_n$ species (n=1 or 3) may form at near ambient conditions, *in-situ* Raman results reveal that it is only the $Pd(H_2)$ species that is

formed in significant amounts at ambient temperature up to 20 bar hydrogen pressure (ESI, Figure S4). This complex has a calculated enthalpy of formation of −83 kJ mol^{-1} H_2 while $PdH_{0.67}$ in 2-3 nm sized Pd nanoparticles forms with an enthalpy in the region of *ca.* –(30-40) kJ mol^{-1} H_2. [29] As the enthalpies of formation highlight it, hydrogen is strongly absorbed in both the Pd(H_2) complex and the interstitial $PdH_{0.67}$, and therefore the hydrogen desorption isotherm of Pd in NH_2-MIL-101(Cr) displays a hysteresis with respect to its absorption (ESI, Figure S5). In addition, it should be noted that, according to Eq. 1, the Pd(H_2) complex is formed *via* the coordination of the hydrogen molecule to the single Pd atom coordinated to the –NH_2 group of the linker and subsequent dissociation from the amino group. Consequently, the desorption takes place from a different species than what is formed during absorption and the two processes thus may not be directly comparable. On this account it is therefore not possible to distinguish the two hydrides based on the analysis of the hydrogen isotherms. However, according to the different absorption enthalpies, the hydrogen desorbed from the two different hydrides could be effectively distinguished thermally and so the proportion of the single atoms could be evaluated.

A method to monitor the controlled desorption of hydrogen from the system as a function of temperature is thermal desorption spectroscopy (TDS). Here, a sample is first loaded with hydrogen, cooled and after the removal of non-adsorbed hydrogen the temperature is increased with a constant heating rate while the quantity of the evolved hydrogen is being measured. [30] This allows a direct correlation to be drawn between the desorption temperature, which is related to the adsorption enthalpy, and the quantity of desorbed hydrogen. It is noteworthy that metal-organic frameworks also adsorb hydrogen through van der Waals interactions. [31] Owing to the chemical complexity of MOFs, adsorption sites of various strength are present in the framework and hydrogen desorption from the NH_2-MIL-101-(Cr) used in this work has been analysed in terms of adsorption sites on the MOF. [21] Since the adsorption enthalpy of hydrogen on Pd nanoparticles and single Pd atoms is significantly higher than those on different MOF sites [31], TDS can be applied to quantify the proportion of single atoms of Pd in the composite of Pd embedded in the NH_2-MIL-101(Cr). It should be noted that the desorption temperature of hydrogen from the interstitial hydride depends on *i)* the size of the Pd nanoparticle, *ii)* the back pressure of the instrument and *iii)* the heating rate applied. [29c;32] Because of this complexity a rigorous scrutiny of previous literature was carried out and it revealed that there is one system directly comparable to the present study [32a], allowing us to assign the peak centred at around 230 K to hydrogen desorption from the interstitial hydride (Figure 2). Note that hydrogen desorption from the interstitial hydride results in two peaks in the TDS spectrum corresponding to the $\beta \rightarrow \alpha$ and β desorption with decreasing temperature. [27c] The peak observed at 230 K is associated with the $\beta \rightarrow \alpha$ transition while the lower-temperature β desorption peak (expected at around 160 K [30a]) overlaps with the higher-intensity

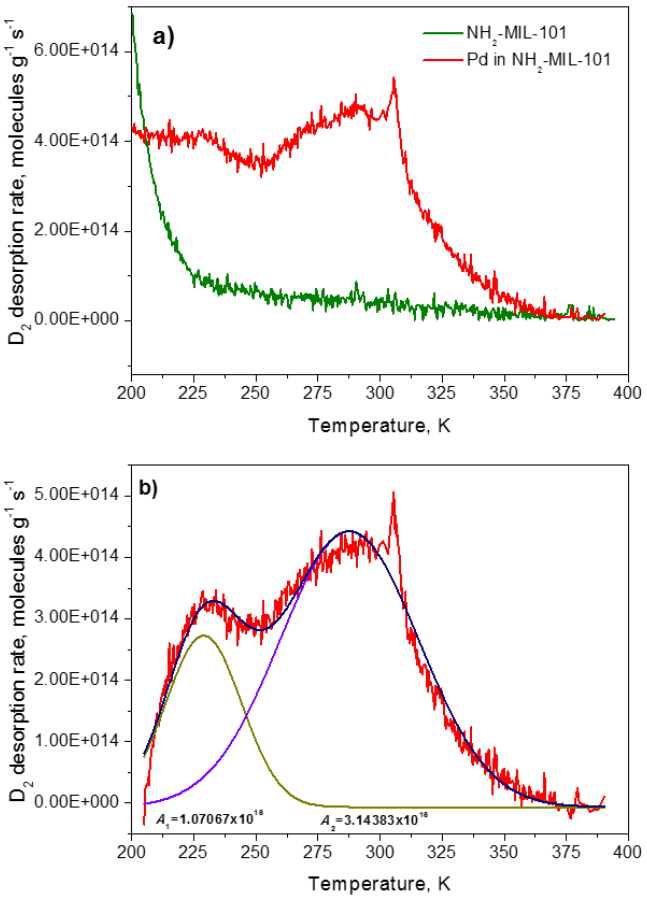

desorption peaks from the MOF scaffold. This means that the desorption peak at 290 K does not arise from desorption from the $PdH_{0.67}$ nanoparticles.

To identify the origin of the desorption peak at 290 K we consider the following; it can be safely excluded that this desorption peak is a consequence of *i)* additional impurity in the framework, *ii)* the reduction of Cr^{3+} in the coordinatively unsaturated sites (CUS, as empirical evidence shows that lower oxidation-state cations in the CUS adsorb hydrogen more

Figure 2 Near ambient-temperature TDS spectra of deuterium from a) the pristine and the Pd containing NH_2-MIL-101 and b) Gaussian fit of the two additional desorption peaks observed in the Pd containing NH_2-MIL-101(Cr) (background signal from the empty MOF subtracted) used for the integration.

strongly [33]) and *iii)* defects in the MOF. The reasons for this are as follows: *i)* all organic residues were removed from the system during hydrogenation at elevated temperatures, and inorganic impurities may only be introduced alongside the Pd precursor albeit with significantly lower concentration; *ii)* XPS results, a very sensitive tool to probe the chemical state of Cr, reveal no oxidation change of the Cr^{3+}-based CUS (ESI, Figure S7), which is in good agreement with previous results obtained on MIL-101(Cr) treated under the same conditions [20]; and *iii)* the strongest binding defects in NH_2-MIL-101(Cr) would be the exposed Cr^{3+} on the CUS through missing or dangling linkers [34] while the desorption temperature of hydrogen from CUS under the same conditions has been previously determined to be 175 K [21] (see also Figure S8, ESI). The assignment of the peak at 290 K to the desorption of hydrogen from the Pd(H_2)

complex is therefore reasonable and the only explanation consistent with the experimental results.

Since the spectrometer was previously calibrated, the number of H atoms or H_2 molecules per gram of sample can be determined by the integration of H_2 desorption peaks. Taking into consideration the hydrogen content of the interstitial $PdH_{0.67}$ hydride and the $Pd(H_2)$ complex, the amount of Pd may be determined from the amount of hydrogen desorbed in each peak. This way we have estimated the number of Pd atoms for 1 g of sample as $6.5x10^{16}$, which is in good agreement with the calculated loading of $1.2x10^{17}$, based on the ICP-OES measurement, and taking into consideration the errors of both ICP-OES and TDS measurements, that of the weighing and the fact that the sample was weighed out in air, which may increase sample mass by over 10% through adsorption. [21]

By integrating the data we were able to determine that a half of the Pd atoms are in the form of single atoms in this system (Figure 2). These results demonstrate that the functionalised MOFs are desirable materials for supporting and stabilising single transition-metal atoms. This observation is also in very good agreement with recent results on the stabilising effect of MOF scaffolds for metastable species. [35]

Conclusions

Metal-organic frameworks are promising materials for the isolation and stabilisation of single atoms of transition metals. In particular, HAADF TEM provided evidence for the immobilisation of single Pd atoms on the NH_2-MIL-101(Cr) framework. Furthermore, taking advantage of the unique spectral features of the $Pd(H_2)$ complex formed on single Pd atoms, TDS enabled us to gauge the proportion of single atoms supported on NH_2-MIL-101(Cr) as 50%. This is a favourable material to be applied as a SAC through its potential to activate hydrogen molecules by significantly elongating the H-H bond.

Experimental

Syntheses.

NH_2-MIL-101(Cr) was synthesised by the chemical reduction of NO_2-MIL-101(Cr) with $SnCl_2$. NO_2-MIL-101(Cr) was obtained by direct hydrothermal synthesis using chromium(III) nitrate $Cr(NO_3)_3.9H_2O$ and 2-nitro-1,4-benzenedicarboxylic acid. [22]

For the infusion of Pd atoms in the MOF's pores, a nominal 5 wt% loading of an acetonitrile solution of the precursor $Pd(CH_3COO)_2$ was used. The precursor Pd^{2+} cations were reduced in a constant 5 V% H_2/Ar flow (5 l/h) at 473 K, for 24 h. For a typical experiment 50 mg MOF was used.

All samples were activated at 433 K under vacuum for 16 h prior to further investigations.

Characterisation.

X-Ray Photoelectron Spectroscopy was carried out using a Thermo Fisher Scientific K Alpha model instrument and the monochromatic Al-K_α radiation (Figure S 3).

Diffuse Reflectance Infra-Red Fourier Transform (DRIFTS) spectra were measured on a Nicolet model 8700 spectrometer, equipped with a high-temperature cell and a DTGS-TEC detector. Samples were pre-treated at 453 K for 1 hour in a helium flow.

Nitrogen adsorption isotherms of the activated samples (Figure S9) were measured on an Autosorb 6B-type nitrogen-adsorption instrument at 77 K.

Hydrogen adsorption and desorption isotherms were measured at 298 and 77 K, in a Sievert's apparatus (HyEnergy, PCTPro-2000) up to *ca.* 30 bar hydrogen pressure. Activated samples were loaded into the microdoser in an Ar glove box.

Elemental analysis was carried out by means of Inductively Coupled Plasma Optical Emission Spectroscopy. The samples were digested in a mixture of 1% HF and 1.25% H_2SO_4. The procedure was carried out *in duplo* with the average taken as result.

Raman spectra were acquired using Bruker Senterra instrument equipped with a 532 nm laser, of 5 cm^{-1} spectral resolution. Samples were added in a crucible then placed into a stainless steel pressure cell equipped with sapphire windows. Typically 20 bar of hydrogen/deuterium was loaded in the cell and spectra were acquired after 30 min to allow the systems to equilibrate.

Thermal Desorption Spectra of H_2, D_2 and the 1:1 H_2-D_2 mixture were acquired using the setup described in. [36] 2-4 mg activated samples (470 K, 3 h, < 10^{-5} mbar) were exposed to 10 mbar of H_2, D_2 or 1:1 H_2-D_2 mixture at 298 K, then slowly cooled down to 20 K. Hydrogen was also loaded in the composite of Pd in NH_2-MIL-101(Cr) at 20 K. The temperature was held for 5 min and the reactor was evacuated. Temperature program of 20-400 K at 0.1 K s^{-1} was finally run. This control allows the circumvention of kinetic effects by setting the heating rate low, *i.e.* near equilibrium conditions. The high sensitivity of the quadrupole mass spectrometer allows to detect amounts of desorbed hydrogen over several orders of magnitude. Quantification of the desorbed hydrogen is possible as the instrument was calibrated with a known standard, as described in reference. [30]

High-angle annular dark-field scanning transmission electron microscopy images were acquired using an aberration-corrected FEI Titan "cubed" microscope, operated in STEM mode at 120 kV acceleration voltage for Fig. 1a-c, with a convergence semi-angle α for imaging of 21.5 mrad and acceptance angle β for HAADF-STEM imaging of 85 mrad, and at 300 kV acceleration voltage for Fig 1d, with α set to 21.5 mrad and β to 50 mrad.

Transmission Electron Tomography data was acquired using a FEI Tecnai microscope, operated in STEM mode at 200 kV using a Fischione single-tilt tomography holder (model 2020). The convergence semi-angle α for imaging was 10 mrad, the acceptance angle β for HAADF-STEM imaging was 90 mrad. Images were acquired every 5 degrees, over a tilt range of -70 to +70 degrees. Reconstruction was performed using a SIRT reconstruction algorithm in the FEI inspect3D software package, visualisation was carried out in the FEI Amira software package.

Computational details.

For the determination of optimised geometries, harmonic vibrational frequencies, and enthalpies and free energies of reaction in the gas phase (at 298.15 K and 1 atm), DFT calculations employed the B3LYP hybrid exchange-correlation functional [37;38] and the aug-cc-pVDZ basis set [39] for H and N atoms, and were performed using the Gaussian 09 Revision A.02 program. [40] For Pd atom the aug-cc-pVDZ-PP basis set [41] was employed, which features an effective core potential (ECP) to describe a 28 electron core, *i.e.* small-core [Ar]3d^{10}. In addition, preliminary calculations using the 6-311++G(2d,2p) [42;43] and SDD [44] basis sets for H and Pd atoms, respectively, were performed for the complexes of Pd with H_2. SDD is an ECP basis set with a 28 electron core for the Pd atom. Geometries for a subset of the complexes with Pd 0 were optimised at the CCSD/6-311++G(2d,2p)/SDD level of theory.
The B3LYP/aug-cc-pVDZ and B3LYP/aug-cc-pVDZ-PP calculations employed a 'tight' geometry optimisation convergence criteria with the Gaussian 09 keywords "opt(tight)" and "int(ultrafine)".

Acknowledgements

The authors would like to acknowledge the help of Sumit Sachdeva in the acquisition of XPS spectra and of Joost Middelkoop in the reactor design. The research was financed by Agentschap.nl (Energy Innovation Funding Agency, #EOSLT07052) the Nanostructured materials for solid-state hydrogen storage COST action (#MP1103), the EPSRC (#EP/N00938X/1) and the EaStCHEM Research Computing Facility for computational resources.

References

1 a) Y. Xia, H. Yang and C. T. Campbell, *Acc. Chem. Res.* **2013**, *46*, 671; b) P. Munnik, P. E. de Jongh and K. P. de Jong, *Chem. Rev.* **2015**, *115*, 6687; c) M. Che and C. O. Bennett, *Adv. Catal.* **1989**, *36*, 55.

2 a) M. Grzelczak, J. Pérez-Juste, P. Mulvaney and L. Liz-Marzán, *Chem. Soc. Rev.* **2008**, *37*, 1783; b) H. Duan, D. Wang and Y. Li, *Chem. Soc. Rev*. **2015**, *44*, 5778; c) M. B. Cortie, and A. M. McDonagh, *Chem. Rev*. **2011**, *111*, 3713; d) J. Kao, K. Thorkelsson, P. Bai, B. J. Rancatore, and T. Xu, *Chem. Soc. Rev*. **2013**, *42*, 2654.

3 a) B. Qiao, A. Wang, X. Yang, L. F. Allard, Z. Jiang, Y. Cui, J. Liu, J. Li and T. Zhang, *Nature Chem*. **2011**, *3*, 634; b) X.-F. Yang, A. Wang, B. Qiao, J. Li, J. Liu and T. Zhang, *Acc. Chem. Res*. **2013**, *46*, 1740; c) S. Liang C. Hao and Y. Shi, *ChemCatChem*, **2015**, *7*, 2559; d) J. Jones, H. Xiong, A. T. DeLaRiva, E. Peterson, H. Pham, S. R. Challa, G. Qi, S. Oh, M. H. Wiebenga, X. I. Pereira Hernández, Y. Wang and A. K. Datye, *Science*, **2016**, *353*, 150.

4 a) A. W. Ehlers, S. Dapprich, S. F. Vyboishchikov and G. Frenking, *Organometallics*, **1996**, *15*, 105; b) P. Achord, E. Fujita, J. T. Muckerman, B. Scott, G. C. Fortman, M. Temprado, X. Cai, B. Captain, D. Isrow, J. J. Weir, J. E. McDonough and C. D. Hoff, *Inorg. Chem.* **2009**, *48*, 7891; c) M. P. Mitoraj and A. Michalak, *Inorg. Chem*. **2010**, *49*, 578; d) M. Mousavi and G. Frenking, *Organometallics*, **2013**, *32*, 1743; e) O. Elbjeirami, S. Yockel, C. F. Campana, A. K. Wilson and M. A. Omary, *Organometallics*, **2014**, *33*, 5101.

5 a) T. E. James, S. L. Hemmingson and C. T. Campbell, *ACS Catal*. **2015**, *5*, 5673; b) A. Figueroba, G. Kovács, A. Bruix and K. M. Neyman, *Catal. Sci. Technol*. **2016**, *6*, 6806; c) F. Dvořák, M. F. Camellone, A. Tovt, N.-G. Tran, F. R. Negreiros, M. Vorokhta, T. Skála, I. Matolínová, J. Mysliveček, V. Matolín and S. Fabris, *Nature Commun*. **2016**, 10801; d) J. Liu, *ACS Catal.* **2017**, *7*, 34.

6 D. Tiana, E. Francisco, M. A. Blanco, P. Macchi, A. Sironi and A. M. Pendás, *J. Chem. Theory Comput*. **2010**, *6*, 1064.

7 J. H. Sinfelt, In *Handbook of Heterogeneous Catalysis*; G. Ertl, H. Knozinger, F. Schüth, J. Weitkamp, Eds.; Wiley-VCH, **1997**, Vol *4*, p. 1939.

8 G. V. Smith and F. Notheisz, In *Heterogeneous Catalysis in Organic Chemistry*, Academic Press: San Diego, CA. **1999**, pp 249.

9 a) S. Kitagawa, R. Kitaura and S. Noro, *Angew. Chem. Int. Ed*. **2004**, *43*, 2334; b) J. L. C. Rowsell and O. M. Yaghi. *Micropor. Mesopor. Mater.* **2004**, *73*, 3.

10 R. L. Martin and M. Haranczyk, *Chem. Sci*. **2013**, *4*, 1781.

11 a) R. Yepez, S. García, P. Schachat, M. Sánchez-Sánchez, J. H. González-Estefan, E. González-Zamora, I. A. Ibarra and J. Aguilar-Pliego, *New J. Chem.* **2015**, *39*, 5112; b) A. M. Bohnsack, I. A. Ibarra, V. I. Bakhmutov, V. M. Lynch and S. M. Humphrey, *J. Am. Chem. Soc.* **2013**, *135*, 16038; c) E. Sánchez-González, A. López-Olvera, O. Monroy, J. Aguilar-Pliego, J. Gabriel Flores, A. Islas-Jácome, M. A. Rincón-Guevara, E. González-Zamora, B. Rodríguez-Molina and I. A. Ibarra, *CrystEngComm*, **2017**, DOI: 10.1039/C6CE02621D.

12 a) H. R. Moon, D.-W. Lim and M. P. Suh, *Chem. Soc. Rev*. **2013**, *42*, 1807; b) A. Dhakshinamoorthy and H. Garcia, *Chem. Soc. Rev*. **2012**, *41*, 5262; c) M. Meilikhov, K. Yusenko, D. Esken, S. Turner, G. Van Tendeloo and R. A. Fischer, *Eur. J. Inorg. Chem*. **2010**, *2010*, 3701; d) C. Rösler and R. A. Fischer, *CrystEngComm*, **2015**, *17*, 199; e) J. Juan-Alcañiz, J. Gascon and F. Kapteijn, *J. Mater. Chem*. **2012**, *22*, 10102; d) A. Corma, H. García and F. X. Llabrés i Xamena, *Chem. Rev.* **2010**, *110*, 4606.

13 a) W. Lu, Z. Wei, Z.-Y. Gu, T.-F. Liu, J. Park, J. Park, J. Tian, M. Zhang, Q. Zhang, T. Gentle III, M. Bosch and H.-C. Zhou, *Chem. Soc. Rev.* **2014**, *43*, 5561; b) X. Kong, H. Deng, F. Yan, J. Kim, J. A. Swisher, B. Smit, O. M. Yaghi and J. A. Reimer, *Science*, **2013**, *341*, 882; c) D. O. Kim, J. Park, G. R. Ahn, H. J. Jeon, J. S. Kim, D. W. Kim, M. S. Jung, S. W. Lee and S. H. Shin, *Inorg. Chim. Acta*, **2011**, *370*, 76; d) M. Eddaoudi, J. Kim, N. Rosi, D. Vodak, J. Wachter, M. O'Keeffe and O. M. Yaghi, *Science*, **2002**, *295*, 469; e) M. Kandiah, S. Usseglio, S. Svelle, U. Olsbye, K. P. Lillerud and M. Tilset, *J. Mater. Chem*. **2010**, *20*, 9848; f) F. A. Almeida Paz, J. Klinowski, S. M. F. Vilela, J. P. C. Tomé, J. A. S. Cavaleiro, J. Rocha, *J. Chem. Soc. Rev*. **2012**, *41*, 1088.

14 a) P. Deria, J. E. Mondloch, O. Karagiaridi, W. Bury, J. T. Hupp and O. K. Farha, *Chem. Soc. Rev.* **2014**, *43*, 5896; b) K. Manna, P. Ji, Z. Lin, F. X. Greene, S. Urban, N. C. Thacker and W. Lin, *Nature Commun*. **2016**, 12610, c) P. Á. Szilágyi, P. Serra-Crespo, I. Dugulan, J. Gascon, H. Geerlings and B. Dam, *CrystEngComm*, **2013**, *15*, 10175.

15 a) R. C. Klet, T. C. Wang, L. E. Fernandez, D. G. Truhlar, J. T. Hupp and O. K. Farha, *Chem. Mater.* **2016**, *28*, 1213; b) H. Zhang, J Wei, J. Dong, G. Liu, L. Shi, P. An, G. Zhao, J. Kong, X. Wang, X. Meng, J. Zhang and J Ye, *Angew. Chem. Int. Ed*. **2016**, *46*, 14310; c) B. Gomez-Lor, E. Gutierrez-Puebla, M. Iglesias, M. A. Monge, C. Ruiz-Valero and N. Snejko, *Inorg. Chem*. **2002**, *41*, 2429; d) N. V. Maksimchuk, M. N. Timofeeva, M. S. Melgunov, A. N. Shmakov, Y. A. Chesalov, D. N. Dybtsev, V. P. Fedin and O. A. Kholdeeva, *J. Catal.* **2008**, *257*, 315.

16 L. Andrews, X. Wang, M. E. Alikhani and L. Manceron, *J. Phys. Chem. A*, **2001**, *105*, 3052; f) J. T. Lyon, H.-G. Cho and L. Andrews, *J. Phys. Chem. A*, **2015**, *119*, 12742.

17 a) I. Luz, C. Rösler, K. Epp, F. X. Llabrés i Xamena and R. A. Fischer, *Eur. J. Inorg. Chem*. **2015**, *2015*, 3904; b) W. Dong, C. Feng, L. Zhang, N. Shang, S. Gao, C. Wang and Z. Wang, *Catal. Lett.* **2016**, 146, 117; c) L. Shen, W. Wu, R. Liang, R. Lin and L. Wu, *Nanoscale*, **2013**, *5*, 9374.

18 D. E. Coupry, J. Butson, P. S. Petkov, M. Saunders, K. O'Donnell, H. Kim, C. Buckley, M. Addicoat, T. Heine, P. Á. Szilágyi, *Chem. Commun*. **2016**, *52*, 5175.

19 M. Latroche, S. Surblé, C. Serre, C. Mellot-Draznieks, P. L. Llewellyn, J.-H. Lee, J.-S. Chang, S. H. Jhung and G. Férey, *Angew. Chem. Int. Ed*. **2006**, *45*, 8227.

20 P. Á. Szilágyi, E. Callini, A. Anastasopol, C. Kwakernaak, S. Sachdeva, R. van de Krol, H. Geerlings, A. Borgschulte, A. Züttel and B. Dam, *Phys. Chem. Chem. Phys.* **2014**, *16*, 5803.

21 P. Á. Szilágyi, I. Weinrauch, J. Juan-Alcañiz, P. Serra-Crespo, A. Grzech, H. Oh, M. de Respinis, B. J. Trześniewski, F. Kapteijn, R. van de Krol, H. Geerlings, J. Gascon, M. Hirscher and B. Dam, *J. Phys. Chem. C*, **2014**, *118*, 19572.

22 S. Bernt, V. Guillerm, C. Serre and N. Stock, *Chem. Commun*. **2011**, *47*, 2838.

23 a) F. Carson , V. Pascanu, A. Bermejo Gómez, Y. Zhang, A. E. Platero-Prats, X. Zou and B. Martín-Matute, *Chem. Eur. J.* **2015**, *21*, 10896; b) V. Pascanu, Q. Yao, A. Bermejo Gómez, M. Gustafsson, Y. Yun, W. Wan, L. Samain, X. Zou and Belén Martín-Matute, *Chem. Eur. J.* **2013**, *19*, 17483.

24 G. F. Svatos, D. M. Sweeny, S.-I. Mizushima, C. Curran and J. V. Quagliano, *J. Am. Chem. Soc*. **1957**, *79*, 3313.

25 a) R. J. T. Houk, B. W. Jacobs, F. El Gabaly, N. N. Chang, A. A. Talin, D. D. Graham, S. D. House, I. M. Robertson and M. D. Allendorf, *Nano Lett.* **2009**, *9*, 3413; b) S. Turner, O. I. Lebedev, F. Schröder, D. Esken, R. A. Fischer and G. Van Tendeloo, *Chem. Mater*. **2008**, *20*, 5622.

26 L. Pauling, In *The nature of the Chemical Bond and the Structure of Molecules and Crystals: An Introduction to Modern Chemistry*, 3rd Edition, Cornell University Press, Ithaca, New York, **1960**, 226.

27 B. Zhang, H. Asakura, J. Zhang, J. Zhang, S. De and N. Yan, *Angew. Chem. Int. Ed*. **2016**, *55*, 8319.

28 a) Y. E. Cheon and M. P. Suh, *Angew. Chem. Int. Ed*. **2009**, *48*, 2899; b) C. Zlotea, R. Campesi, F. Cuevas, E. Leroy, P. Dibandjo, C. Volkringer, T. Loiseau, G. Férey and M. Latroche, *J. Am. Chem. Soc.* **2010**, *132*, 2991; c) M. Sabo, A. Henschel, H. Fröde, E. Klemm and S. Kaskel, *J. Mater. Chem*. **2007**, *17*, 3827.

29 a) M. Johansson, E. Skúlason, G. Nielsen, S. Murphy, R. M. Nielsen and I. Chorkendorff, *Surf. Sci.* **2010**, *604*, 718; b) M. Yamauchi, R. Ikeda, H. Kitagawa and M. Takata, *J. Phys. Chem. C*, **2008**, *112*, 3294; c) V. A. Vons, H. Leegwater, W. J. Legerstee, S. W. H. Eijt and A. Schmidt-Ott, *Int. J. Hydr. Energy*, **2010**, *35*, 5479; d) S. Syrenova, C. Wadell, F. A. A, Nugroho, T. A. Gschneidtner, Y. A. Diaz Fernandez, G. Nalin, D. Świtlik, F. Westerlund, T. J. Antosiewicz, V. P. Zhdanov, K. Moth-Poulsen, C. Langhammer, *Nature Mater.* **2015**, *14*, 1236; e) R. Gremaud, C. P. Broedersz, D. M. Borsa, A. Borgschulte, P. Mauron, H. Schreuders, J. H. Rector, B. Dam, and R. Griessen, *Adv. Mater.* **2007**, *19*, 2813.

30 F. von Zeppelin, M. Haluška and M. Hirscher, *Thermochim. Acta*, **2003**, *404*, 251.

31 a) D. Zhao, D. Yuan and H. C. Zhou, *Energy Environ. Sci.* **2008**, *1*, 222; b) L. J. Murray, M. Dincă and J. R. Long, *Chem. Soc. Rev.* **2009**, *38*, 1294; c) J. Sculley, D. Yuan and H.-C. Zhou, *Energy Environ. Sci*. **2011**, *4*, 2721; d) A. F. Kloutse, R. Zacharia, D. Cossement, R. Chahine, R. Balderas-Xicohténcatl, H. Oh, B. Streppel, M. Schlichtenmayer and M. Hirscher, *Appl. Phys. A*, **2015**, *121*, 1417.

32 a) R. Campesi, F. Cuevas, R. Gadiou, E. Leroy, M. Hirscher, C. Vix Guterl and M. Latroche, *Carbon*, **2008**, *46*, 206; b) C. Zlotea, F. Cuevas, V. Paul-Boncour, E. Leroy, P. Dibandjo, R. Gadiou, C. Vix-Guterl and M. Latroche, *J. Am. Chem. Soc*. **2010**, *132*, 7720; c) J. F. Fernández, F. Cuevas and C. Sánchez, *J. Alloys & Comp.* **2000**, *298*, 244; d) M. Morkel, G. Rupprechter and H.-J. Freund, *Surf. Sci*. **2005**, *588*, L209.

33 C. K. Brozek and M. Dincă, *Chem. Soc. Rev*. **2014**, *43*, 5456.

34 a) J. Ren, H. W. Langmi, N. M. Musyoka, M. Mathe, X. Kang and S. Liao, *Mater. Today*, **2015**, *2*, 3964; b) P. Á. Szilágyi, P. Serra-Crespo, J. Gascon, H. Geerlings and B. Dam, *Front. Energy Res*. **2016**, *4*, 9.

35 E. Callini, P. Á. Szilágyi, M. Paskevicius, N. P. Stadie, J. Réhault, C. E. Buckley, A. Borgschulte and A. Züttel, *Chem. Sci*. **2016**, *7*, 666.

36 B. Panella, M. Hirscher and B. Ludescher, *Micropor. Mesopor. Mater*. **2007**, *103*, 230.

37 A. D. Becke, *J. Chem. Phys.* **1993**, *98*, 5648.

38 P. J. Stephens, F. J. Devlin, C. F. Chabalowski and M. J. Frisch, *J. Phys. Chem*. **1994**, *98*, 11623.

39 T. H. Dunning, *J. Chem. Phys*. **1989**, *90*, 1007.

40 M. J. Frisch, G. W. Trucks, H. B. Schlegel, G. E. Scuseria, M. A. Robb, J. R. Cheeseman, G. Scalmani, V. Barone, B. Mennucci, G. A. Petersson, H. Nakatsuji, M. Caricato, X. Li, H. P. Hratchian, A. F. Izmaylov, J. Bloino, G. Zheng, J. L. Sonnenberg, M. Hada, M. Ehara, K. Toyota, R. Fukuda, J. Hasegawa, M. Ishida, T. Nakajima, Y. Honda, O. Kitao, H. Nakai, T. Vreven, J. A. Montgomery Jr., J. E. Peralta, F. Ogliaro, M. Bearpark, J. J. Heyd, E. Brothers, K. N. Kudin, V. N. Staroverov, R. Kobayashi, J. Normand, K. Raghavachari, A. Rendell, J. C. Burant, S. S. Iyengar, J. Tomasi, M. Cossi, N. Rega, J. M. Millam, M. Klene, J. E. Knox, J. B. Cross, V. Bakken, C. Adamo, J. Jaramillo, R. Gomperts, R. E. Stratmann, O. Yazyev, A. J. Austin, R. Cammi, C. Pomelli, J. W. Ochterski, R. L. Martin, K. Morokuma, V. G. Zakrzewski, G. A. Voth, P. Salvador, J. J. Dannenberg, S. Dapprich, A. D. Daniels, Ö. Farkas, J. B. Foresman, J. V. Ortiz, J. Cioslowski, J. and D. J. Fox, Gaussian 09, Revision A.02, Gaussian, Inc., Wallingford CT, **2009**.

41 K. A. Peterson, D. Figgen, M. Dolg, and H. Stoll, *J. Chem. Phys*. **2007**, *126*, 124101.

42 R. Krishnan, J. S. Binkley, R. Seeger and J. A. Pople, *Chem. Phys*. **1980**, *72*, 650.

43 M. J. Frisch, J. A. Pople and J. A. Binkley, *J. Chem. Phys*. **1984**, *80*, 3265.

44 D. Andrae, U. Häussermann, M. Dolg, H. Stoll and H. Preuss, *Theor. Chim. Acta*, **1990**, *77*, 123.